ANL/ER/CP-103067

THE USE OF ROTATING SHADOWBAND RADIOMETERS AND MICROWAVE RADIOMETERS TO OBTAIN CLOUD PROPERTIES IN ARCTIC ENVIRONMENTS

by

James C. Barnard
Pacific Northwest National Laboratory
Richland, Washington

James C. Liljegren*
Environmental Research Division
Argonne National Laboratory
Argonne, Illinois

Qi-Long Min
Atmospheric Sciences Research Center
State University of New York
Albany, New York

J. C. Doran
Pacific Northwest National Laboratory
Richland, Washington

for submission to

11th Symposium on Meteorological Observations and Instrumentation,
14-19 January 2001, Albuquerque, New Mexico.

*Work at Argonne National Laboratory was supported by the U.S. Department of Energy, Office of Science, Office of Biological and Environmental Research, Environmental Sciences Division, under contract W-31-109-Eng-38.

DISCLAIMER

6.4

THE USE OF ROTATING SHADOWBAND RADIOMETERS AND MICROWAVE RADIOMETERS TO OBTAIN CLOUD PROPERTIES IN ARCTIC ENVIRONMENTS

J. C. Barnard*
Pacific Northwest National Laboratory, Richland, Washington
J. C. Liljegren
Argonne National Laboratory, Argonne, Illinois
Qi-Long Min
Atmospheric Sciences Research Center, State University of New York, Albany, New York
J. C. Doran
Pacific Northwest National Laboratory, Richland, Washington

1. INTRODUCTION

The multi-filter rotating shadowband radiometer (MFRSR; Harrison et al., 1994) and the microwave radiometer (MWR; Liljegren, 1994) are mainstays in the Atmospheric Radiation Measurement (ARM) Program's suite of radiometric instrumentation. The MFRSR measures direct normal radiation, diffuse radiation, and total radiation at six distinct wavelengths (415 nm, 500 nm, 615 nm, 673 nm, 870nm, and 940 nm) with a passband of about 10 nm. Additionally, broadband shortwave radiation is measured using a silicon photodiode. From the MFRSR measurements one can derive a wealth of information regarding the optical state of the atmosphere including aerosol and cloud optical depths. From the MWR one can measure columnar water vapor and liquid water path (LWP). When the MFRSR measurements are combined with those from the MWR, it becomes possible to calculate the cloud droplet effective radius as well.

The MWR and MFRSR were deployed at the SHEBA ice camp from October 1997 until October 1998. (SHEBA stands for Surface Heat Budget of the Arctic Ocean, see http://sheba.apl.wahsington.edu) Since early 1998 an MWR and an MFRSR have also been deployed at the ARM Barrow site. The presence of these instruments in the Arctic presents a unique opportunity to investigate the spatial and temporal distribution of aerosol and cloud optical depth as well as evaluate the performance of these instruments in the inhospitable arctic environment. In this paper we discuss some of the issues associated with instrument deployment in the arctic environment as well as some preliminary results derived from measurements taken at the two sites.

*Corresponding author address: Jim Barnard, Pacific Northwest National Laboratory, MSIN: K9-30, Richland, WA 99352; e-mail: james.barnard@pnl.gov

2. ISSUES RELATED TO INSTRUMENT DEPLOYMENT IN THE HARSH ARCTIC ENVIROMENT

Prior to the installation of the instruments in the Arctic it was thought that the very cold temperatures posed the biggest threat to success of the instruments' operation. This concern did not prove to be true because the usual cold weather by itself seemed to cause few if any problems*. However, other unanticipated difficulties arose from the fact that the SHEBA MFRSR was mounted aboard a ship frozen in the ice, and the constant twisting of the ice floe led to frequent alignment problems with the MFRSR. Additionally, for unknown reasons the data emanating from the instrument were unusually noisy, and special measures were necessary to remove this noise. The use of the instruments at the Barrow site was and remains relatively uncomplicated except for the determination of the surface albedo during the snowmelt that occurs in late May and early June. There also have been concerns expressed about the calibration and retrieval procedures used for the MWR, but a recent evaluation of the MWR performance suggests that the instrument worked well (Han et al., 2000).

2.1 *MFRSR Alignment Problems at the SHEBA Site*

A sample of the MFRSR data from the SHEBA site is shown in Figure 1. This figure illustrates the effect on the data of the misalignment problem mentioned above. The instrument uses a shadowband to shade the detector; while such shading take place a reading of the diffuse irradiance is possible. If the instrument is not oriented correctly -- it must be facing true north -- then the shadowband may not fully shade the radiation sensor during the shading phase of the measurements. This partial shading leaves an imprint on the data and is vividly apparent in Figure 1 as the fuzziness in these data from about 7 to 12 hours (local standard time, LST). Additionally, there is a slight shading problem from about 23 to 24 hours (LST) although this is difficult

*Extremely cold weather -- at the low end of the seasonal temperature range -- did cause some instrument operation problems.

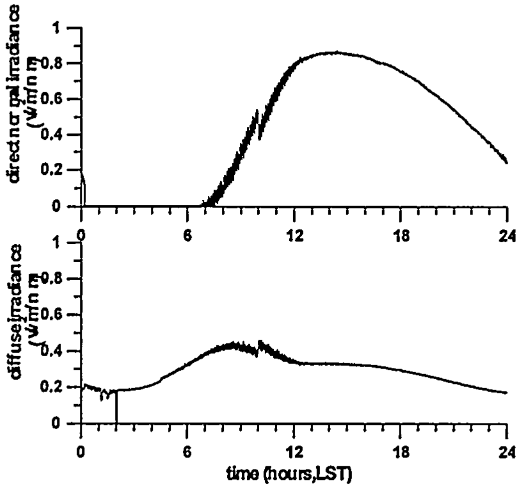

Figure 1: Direct normal and diffuse irradiances (415 nm) from the SHEBA MFRSR (1998/06/23). The misalignment problem is illustrated by the fuzziness in these data from about 7 to 12 LST and 23 to 24 LST. The "notch" in these data that occurs around 10 LST is perhaps an indication of an effort to align the instrument.

to see in the figure. If the sun is not completely blocked by clouds so that some direct beam radiation strikes the detector then the shading problem renders both the direct normal irradiance and the diffuse irradiance nearly useless. If, however, there is virtually no direct beam radiation impinging on the sensor, then we may regard the direct beam as zero and the shading problem becomes irrelevant because the shadowband will have no direct beam radiation to block. In this case the diffuse radiation is measured correctly and it is identical to the total radiation. We again emphasize here that the degradation of these data are not the fault of the instrument but is caused by the twisting of the ship on which the MFRSR resides.

If any direct beam was present while the instrument was in the misaligned state, it was not possible to recover either the direct beam or diffuse radiation. However, we developed a procedure that could identify these periods and cull them from the data set prior to the optical depth retrievals. This procedure uses the MFRSR's broadband diffuse irradiance and compares this irradiance with measurements from the shaded pyranometers on board the SHEBA ship. Because the shaded pyranometers were correctly shaded for most (but not all) of the SHEBA experiment, shading problems with the MFRSR showed up markedly in this comparison. Figure 2 shows an example from 1998/06/23 – the same day as Figure 1. In Figure 2 the diffuse broadband irradiance from the MFRSR has been plotted as the solid line while the dashed line is the diffuse irradiance from the shaded pyranometer. (This irradiance has been multiplied by a factor of 0.75 so that it "lines up" with the MFRSR data. This factor accounts for possible calibration differences between the instruments and the fact that the MFRSR broadband detector is a silicon photodiode and does not have a flat frequency response across the shortwave spectrum.)

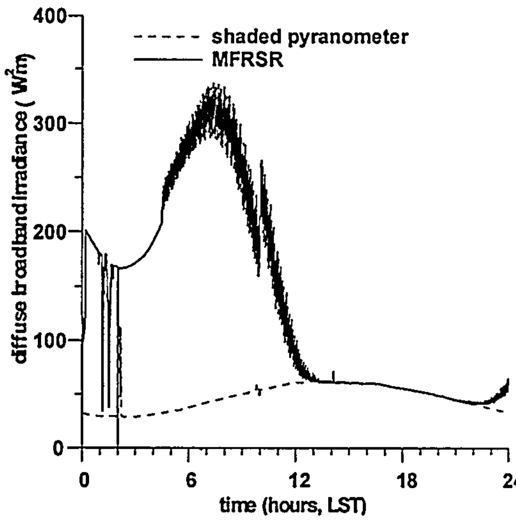

Figure 2: Diffuse broadband irradiances from the MFRSR (solid line) and shaded pyranometer (dashed line) for 1998/06/23.

As shown in Figure 2 the discrepancy between the two irradiances is very large throughout most of the day, except between the hours of about 1400 LST to about 2300 LST. During this interval the irradiances match up quite well. This congruence suggests that the MFRSR was aligned well during this period and that data outside this time period is faulty and cannot be used in our optical depth calculations. A similar analysis applied to the rest of the SHEBA data between June 1, 1998 and September 30, 1998 revealed that about 20% of the data were bad. We were fortunate the so much data were recoverable considering the difficult conditions under which the MFRSR was operated.

2.2 *MFRSR Noise Problems at the SHEBA Site*

For lengthy periods of time the MFRSR data from the SHEBA ice camp also suffered from noise problems. We not know from whence these problems arose; regardless of the origin of the noise, it was desirable to remove it when it occurred. An example of the noise is shown in Figure 3 for 415 nm diffuse data recorded on 1998/05/26. The 415 nm channel is particularly important for this study because it is from this wavelength channel that cloud optical depths are derived. The top graph in figure – labeled "unfiltered data" – is the original data before processing to remove the noise. In this time series low-amplitude, high-frequency noise permeates the entire time series. A Wiener optimal filter (Press et al., 1992) was designed to remove this noise while retaining as much of the signal as possible (hence the appellation "optimal" filter). The result of running the filter through the time series is shown in the bottom "trace" of Figure 3 where this trace has been displaced downward for clarity. A visual examination indicates that the filter seems to be doing the job it was designed to do: reduce noise while minimally affecting the signal. Visual inspection of the filtered data over many other time periods strengthens this conclusion.

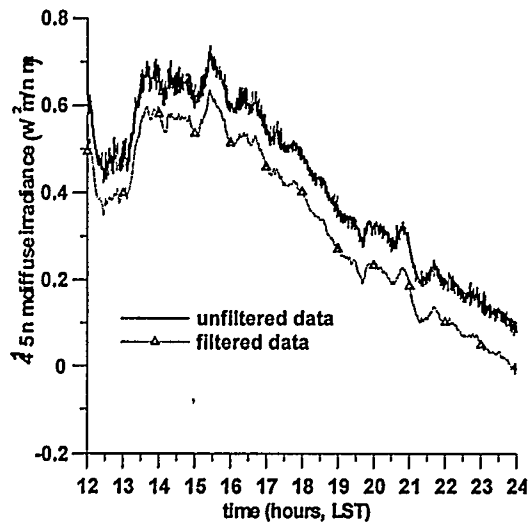

Figure 3: Filtered and unfiltered diffuse irradiance data, 415 nm, from 1998/05/26. The graph representing the filtered data has been displaced 0.1 units downward for clarity.

2.3 *MFRSR Calibration*

Accurate MFRSR calibration is crucial to obtain accurate estimates of cloud properties. We were fortunate that during the SHEBA campaign there were enough clear days to permit the calibration of the instrument to be monitored and corrected using the Langley method (see Harrison and Michalsky, 1994). Although the initial calibration (i.e., the calibration prior to deployment) of the 415 nm channel appeared to be in error by about 13%, the calibration appeared to remain stable throughout the period of interest (June through September 1998). Correcting the calibration was therefore just a matter of multiplying the data by a constant factor.

Once the SHEBA MFRSR data have been reviewed to remove bad data, filtered to reduce noise, and then calibrated, we then have good quality data on hand from which we may calculate cloud optical depths. However, to obtain effective radius as well as cloud optical depth, we must add liquid water path (LWP) as an input variable to our calculations. The inclusion of LWP also enhances the physical verisimilitude of the optical depth calculations because information about the effective radius may be inferred from the data (as opposed to assuming a plausible effective radius for the calculations). The LWP is obtained from the MWR installed at the SHEBA site. These data, too, must be reviewed to detect and eliminate bad measurements.

2.4 *Microwave Radiometer data processing to remove spikes in LWP*

The LWP data taken from the MWR is sometimes contaminated by water residing on the cover that protects the MWR optics. The source of such water is usually precipitation. A moisture sensor placed near the optics cover can detect precipitation and data taken during known precipitation events can be flagged and thrown out. This approach is somewhat crude and does not completely eliminate contamination. To better distinguish between contaminated and uncontaminated data an algorithm has been developed by J. Liljegren that uses a filtering technique to detect contaminated data.

We will not describe the algorithm here but instead illustrate the results of its application. Often the precipitation events leading to contamination are brief and can be identified by a "spike" in the LWP. Figure 4 illustrates such a spike. This feature was identified by the algorithm and then flagged. (By our convention a flag equal to zero indicates a good measurement; a value equal to one means bad data). It was not possible to calculate cloud effective radius for time periods during which the MWR data was determined to be of poor quality.

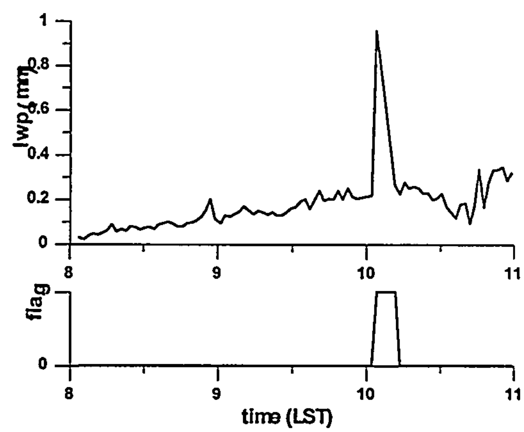

Figure 4: LWP as measured from the SHEBA MWR on 1999/08/15 (upper panel). The spike in the LWP that occurs close to 10 AM represents contaminated data and the flag (in the lower panel) has been set equal to one indicating bad data

3. CLOUD OPTICAL DEPTH CALCULATIONS

Once bad data have been culled from the MFRSR and MWR data sets we can calculate cloud optical depth. For these calculations we used the algorithm developed by Min and Harrison (1996). In brief (and oversimplified) terms this algorithm uses diffuse transmission at 415 nm to infer cloud optical depth: the less the transmission the greater the cloud optical depth. The algorithm takes as input the diffuse, direct normal, and total irradiances at 415 nm and the LWP from the MWR. The algorithm then produces cloud optical depth, τ, and cloud droplet effective radius, r_e.

Cloud optical depth and effective radius are calculated and stored as 5-minute averages. Figures 5 and 6 show examples of a daily time series of τ and r_e, respectively, for 1998/07/23 at the SHEBA site.

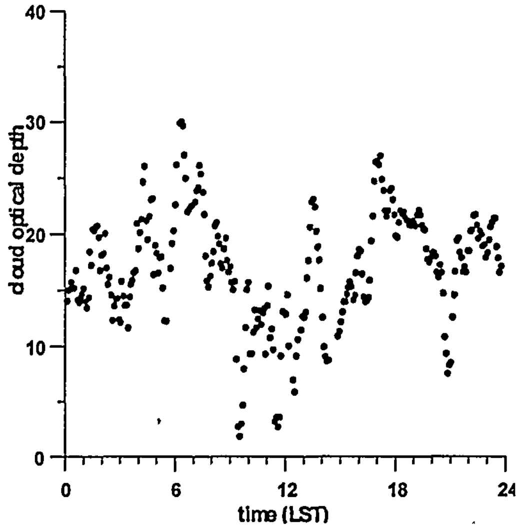

Figure 5: Cloud optical depth calculated from the Min and Harrison (1996) algorithm for the SHEBA ice camp, 1998/07/23.

Figure 5 reveals that for this day the cloud optical depth varied from a low of about 5 to a high about 30 over a 24-hour period. The mean and median optical depths were about 17. The fact that the sun was up during the entire day at this site permitted optical depth calculations to be performed throughout the entire 24 hours of the day; this is one of the few advantages of a high latitude site!

Effective radii are shown in Figure 6. For this 24 hour time span, the median and mean radii were 6.8 and 8.0 microns, respectively with 25% and 75% quartiles of 5.7 and 8.5 microns, respectively. Although taken from a single day, these statistics are close to those reported by Herman and Curry (1984). In their study the median effective radius -- derived from aircraft measurements -- was found to be 7.3 microns, and the 25th and 75th quartiles were 5.8 and 8.2, respectively. Such agreement can only bolster confidence in the measurements and calculations described here.

The results presented above merely illustrate typical daily time series for τ and r_e. For a more comprehensive view of these data, we show in Table 1 the median values of the cloud optical properties derived from the SHEBA and Barrow MFRSRs for the "Summer" season (June through September) 1998, and also for the same season during 1999 at Barrow. For the 1998 season at Barrow, the MWR was not fully operational and we could not derive cloud effective radii.

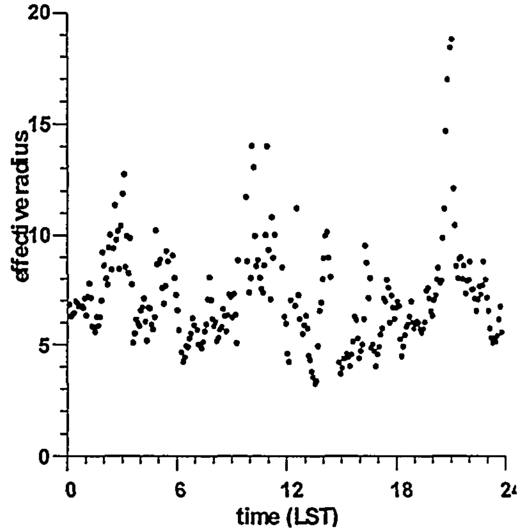

Figure 6: Cloud effective radii, r_e, calculated for 1998/07/23.

Site	τ	r_e(microns)
SHEBA - 1998	19.6	7.5
Barrow - 1998	14.3	—
Barrow - 1999	10.4	13.1

Table 1: Median values of cloud optical depth, τ, and cloud droplet effective radius, r_e, for the SHEBA and Barrow sites for the years indicated.

That the shortwave optical depth at all the two sites is relatively small is consistent with other measurements of the optical depth of arctic stratus clouds. For example, Leontyeva and Stamnes (1994) used broadband pyranometers to infer cloud optical depth at Barrow, Alaska and their results indicate an average optical depth over the summer months (excluding September) of about 15. Our measurements show a median optical depth of 10 and 14 for the two seasons at Barrow (including September) and this range of optical depths is reasonably consistent with the findings of Leontyeva and Stamnes.

The results shown in this table imply a difference between cloud properties at Barrow and at the position of the SHEBA ice camp. We are now preparing a manuscript in which a much more detailed exposition of these results will be provided.

4. CONCLUSIONS

Measurements taken from MFRSRs and MWRs at the SHEBA ice camp and the ARM Barrow site have been used to derive cloud optical depth and cloud droplet effective radius at these sites. The SHEBA MFRFR was operated in particularly difficult circumstances under which the instrument suffered from noise and alignment problems. Techniques were devised to identify these problems and either correct them (in the case of noise) or simply remove bad data from consideration. The values of τ and r_e derived from this analysis seem reasonable and are consistent with other measurements. This agreement suggests that the instruments were functioning well during the SHEBA campaign. The Barrow instruments performed well during the time periods considered in this paper, and the Barrow instruments continue to function well up to the present time.

5. REFERENCES

Han, Y., E. R. Westwater, M. Shupe, and S. Y.Matrosov, 2000: Analysis of Integrated Cloud Liquid and Precipitable Water Vapor Retrievals from Microwave Radiometers during SHEBA. Submitted to *J. Geophys. Res.*

Harrison. L., J. Michalsky, and J. Berndt, 1994: Automated multifilter rotating shadowband radiometer: An instrument for optical depth and radiation measurements. *Appl. Opt.*, **33**, 5118-5125.

Harrison, L. and J. Michalsky, 1994: Objective algorithms for the retrieval of optical depths from ground-based measurements. *Appl. Opt.*, **33**, 5126-5132.

Herman, G. F. and J. A. Curry, 1984: Observational and theoretical studies of solar radiation in Arctic stratus clouds. *J. Climate Appl. Meteor.*, **23**,5-24.

Leontyeva, E. and K. Stamnes, 1994: Estimations of cloud optical thickness from ground-based measurements of incoming solar radiation in the Arctic. *J. Climate*, **7**, 566-578.

Liljegren, J., 1994: Two-channel microwave radiometer for observations of total column precipitable water vapor and cloud liquid water path. *Fifth Symposium on Global Change Studies*, January 23-28, Nashville, Tennessee.

Min, Q. and L. Harrison, 1996: Cloud properties derived from surface MFRSR measurements and comparison with GOES results at the ARM SGP site. *Geophys. Res. Lett.*, **23**, 1641-1644.

Press, W. H., S. A. Teukolsky, W. T. Vetterling, and B. P. Flannery, 1992: *Numerical Recipes. The Art of Scientific Computing*. 2d ed. Cambridge University Press, 961 pp.

Acknowledgement

This research was sponsored by the U. S. Department of Energy under Contract DE-AC06-76RLO 1830 at Pacific Northwest National Laboratory. Pacific Northwest National Laboratory is operated for the U. S. Department of Energy by Battelle Memorial Institute. The ARM Program is sponsored by the U. S. Department of Energy.